An experimental investigation of a two-layer inviscid shock cap due to blunt-body nose injection

By JUDSON R. BARON AND EDGAR ALZNER
Aerophysics Laboratory, Massachusetts Institute of Technology

(Received 30 August 1962)

Blunt-body solutions for suspersonic flow usually concern closed body surfaces. This paper reports on an experimental investigation of a two-layer shock cap and indicates the existence of a predictable contact surface separating the layers. The inner layer was generated by injecting air through a contoured axisymmetric channel on a blunt body so as to simulate a hemispherical contact surface in a Mach number 4·8 flow.

Results show the existence of the contact surface and the influence of a range of mass-injection rates upon the displacement of the bow shock and contact surface from the body.

1. Introduction

The problem of aerodynamic heating has suggested the use of blunt bodies and injection cooling schemes as thermal protective devices. One such method consists of an upstream-directed jet emanating from the stagnation region of the body. The coolant flow is then diverted rearward by the action of the oncoming stream and can alter the physical properties in a 'buffer' layer immediately adjacent to the body. As in transpiration cooling the coolant fluid is arbitrary and its state may be controlled independently. In addition, the directed-jet approach includes possible effects on the inviscid shock-layer field.

Both McMahon (1958) and Warren (1960) have studied the directed-jet effects upon pressure and heat-transfer distributions and flow patterns. Apparently for 'large' injection rates the bow shock wave is deformed and results in a shift in the location of the severest heat-transfer rates to a stagnation 'circle'. For 'low' injection rates the shock layer is virtually undisturbed and heat-transfer reductions may be related to the heat capacity of the injectant employed.

The emphasis in previous investigations has been largely phenomenological. The presence of separated flow regions has prohibited an analytical approach whereas even without gross separation the injection rates were somewhat greater than those applicable to transpiration cooling of the viscous layer. Coolants have been introduced through arbitrary passages with axisymmetry alone provided as a match to the test geometries. The present work describes an experimental investigation of a predicted two-layer flow field lying between the bow shock and a blunt body. One may infer the analogy to a source distribution in a uniform incompressible flow. The inner, or buffer, layer is comprised of injected material. Although the ultimate purpose is thermal protection of the body we consider only the inviscid flow-field geometry here.

2. Basis for two-layer model

Both inverse and direct evaluations have been employed to determine shock-cap geometry and flow description. One starts with a known boundary, shock or body, and seeks a subsonic flow field which satisfies proper conditions at a secondary boundary, i.e. body or shock. It is clear that any streamline is a permissible starting point and that existing high-speed-flow solutions have

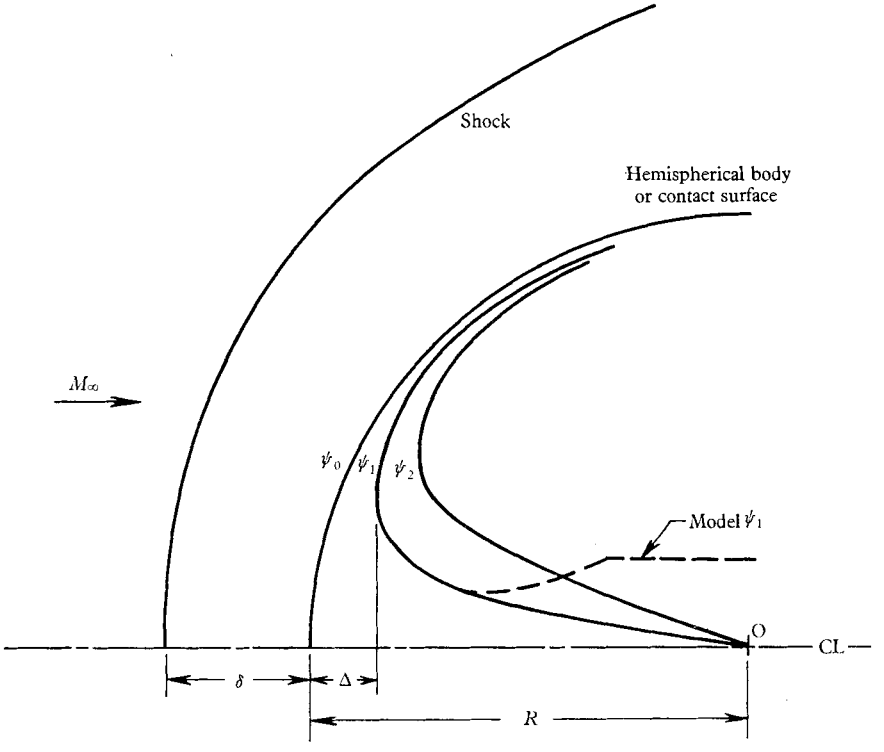

FIGURE 1. Model geometry illustrating streamline choices for hemispherical body (ψ_0) or hemispherical contact surface (ψ_1, ψ_2).

tacitly assumed an interest in 'solid' bodies. Figure 1 illustrates the streamline pattern interior to a (hemispherical) blunt body and supposing a reverse flow (from the source O) such that the body skin remains a streamline. With such a reverse flow the original body surface can be thought of as a contact surface separating inner and outer layers of fluid. Contact surface displacement distances (Δ in figure 1) proved to be of the same order as the original shock displacement distances (δ in figure 1) for reasonable mass flows.

Martin (1958) considered only the ψ_0 geometry but his work permits evaluation of the 'interior' streamlines and flow field as well. Based on an (x, y)-coordinate system measured along and normal to the hemispherical contact surface the stream function is defined as

$$\psi_y = \rho u(1+Ky)\sin Kx/K, \quad \psi_x = -\rho v(1+Ky)^2 \sin Kx/K; \tag{1}$$

u and v are velocity components in the x and y directions and K is the local curvature. Substitution of ρu and ρv from equation (1) into the continuity equation results in a differential equation for the stream function and a solution of the form

$$\psi = (\rho_\infty \sin^2\theta/kK) f(y), \tag{2}$$

where

$$f(y) = \{A(1+Ky)^4 + B(1+Ky)^2 + C(1+Ky)^{-1}\}\, ku_\infty/K \tag{3}$$

and

$$\left.\begin{aligned} A = \tfrac{1}{10}\alpha^2(1+K\delta)^{-2}, \quad B = \tfrac{1}{6}(3+2\alpha-\alpha^2), \quad C = \tfrac{1}{15}\alpha(1+K\delta)^3(\alpha-5), \\ \alpha = (1-k)/k, \quad k = \rho_\infty/\rho. \end{aligned}\right\} \tag{4}$$

A specific internal flow is implied for a given set of main-stream conditions. The appropriate injectant flow rate follows from consideration of the mass flux contained within a cylinder concentric with the body axis, i.e.

$$\dot{m} = \rho_\infty u_\infty \{\pi(R+\delta)^2 \sin^2\theta\}, \tag{5}$$

where R is the hemispherical radius (see figure 1). Eliminating θ by evaluating ψ for $f(\delta)$ results in

$$\dot{m} = \left\{\frac{\rho_\infty u_\infty^2 k}{f(\delta)\, K}\, \pi R^2 \left(1+\frac{\delta}{R}\right)^2\right\} \psi^*, \tag{6}$$

if $\psi^* = (K^2/\rho_\infty u_\infty)\psi$ is introduced as a dimensionless mass-flow parameter. A choice of Δ/δ results in a specific ψ^*, i.e. ψ_i^*, and thus the necessary coolant supply rate.

For inviscid flow only the pressure distribution must be matched along the contact surface which implies that the injectant should be supplied with a stagnation pressure corresponding to that after a normal shock in the main stream. The development of equation (2) is based upon the assumption of a constant-density flow and the simplicity of the result justifies its use for this preliminary investigation.

3. Description of experiment

The experiments were conducted in the 4×4 in. free jet hypersonic circuit at the Aerophysics Laboratory of the Massachusetts Institute of Technology. The stagnation temperature of 1360 °R and nominal Mach number of 4·8 correspond to a free-stream Reynolds number equal to $1{\cdot}05 \times 10^5$ per inch.

A total of six models were provided with two base diameters (0·8 and 1·2 in.) and three surface boundaries (ψ_0, ψ_1, and ψ_2). All conformed to a predicted hemispherical contact surface (i.e. ψ_0) in the shock layer. No instrumentation was present within the models. Upstream injection originated from air pressure flasks, such that after passage through a pressure regulator, the air was metered through a sonic orifice outside the test channel. Stagnation pressure and temperature at a sonic orifice were measured using a Heise gauge and thermocouple arrangement, and mass flow rate was inferred from prior calibration of the orifice. A needle valve upstream of the orifice furnished mass flow-rate control.

A consequence of the constant-density-source flow basis (Martin 1958) for the chosen ψ_i was very large velocities and corresponding low pressures in the vicinity of O (figure 1). Along the model axis the predicted pressure distribution

decreases to 'sonic' pressure at about a quarter-radius from the stagnation point, with virtually little change in the location for the ψ_i considered here. In order to avoid supersonic diffusion the injectant channels were arbitrarily faired into circular entry tubes so as to maintain a subsonic flow throughout the model interior. The dashed contour in figure 1 illustrates the actual ψ_i line as typical of the construction.

During the test, shadowgraph pictures were obtained at successive mass flow rates of the injected air through a range including the design condition. For each injection and solid (ψ_0) model pictures were also obtained without injection.

For the test the conditions were: $u_\infty = 3665$ ft./sec, $k = 0{\cdot}203$, $K = 30$ and 20/ft., $\delta_D/R = 0{\cdot}143$, so that $\dot{m} = 48{\cdot}84R^2\psi^*$ lb./sec with $[R]$ = ft. Table 1 lists

Model	Base diameter (in.)	ψ^*	$\dot{m}_D$ (lb./sec)
1*a*	1·2	0	0
1*b*	1·2	0·007	0·000855
1*c*	1·2	0·014	0·001710
2*a*	0·8	0	0
2*b*	0·8	0·007	0·000380
2*c*	0·8	0·014	0·000760

TABLE 1.

the models tested. For comparison with Warren (1960) note that a mass flow coefficient $C_{\dot{m}} = \dot{m}/\rho_\infty u_\infty \pi R^2 = 2{\cdot}0\psi^*$. His data were obtained for $C_{\dot{m}} \leqslant 0{\cdot}008$ in contrast to the values of 0·014 and 0·028 in these tests.

4. Results

Figure 2*a*, *b*, *c*, plate 1, show the basic range of flow patterns for the original (ψ_0) and $\psi^* = 0{\cdot}007$ models (1*a*, *b*) with overblown and no injection rates ($\dot{m}/\dot{m}_D = 0$, 1·40). In the absence of injection no contact surface is present and the flattening of the bow shock is not easily discernible. The contact surface is also missing from figure 2*c*, indicating a rather substantial mixing process. This may in part be related to a high frequency unsteadiness observed in some overblown cases.

A series of injection rate flow patterns is shown in figure 3*a–f*, plates 2 and 3, for model 1*c*. Here the contact surface and its increasing displacement distance are clearly visible. The last (figure 3*f*) of this sequence is actually one of an oscillatory flow pattern. Only one such overblown picture is reproduced here since the others are qualitatively identical and exhibit only relative (and small) displacements of the shock and contact surfaces. It is interesting that over a wide range of flow rates a nearly spherical contact surface results. Even for the overblown cases (figures 2*c*, 3*f*) the major influence on the flow field is confined within an angle of about 45° from the axis.

Measurements of shock and contact-surface displacement distances (δ, Δ) were made from the shadowgraph negatives and referred to design values

(δ_D, Δ_D). The results are shown in figures 4 and 5. Martin (1958) predicts the value $\delta_D/R = 0{\cdot}143$ used here and justified on the experimental basis of $0{\cdot}15 \pm 0{\cdot}01$ and $0{\cdot}12 \pm 0{\cdot}02$ for models $1a$, $2a$, respectively. Δ_D/R follows from the geometry as 0·0654 and 0·0921 for $\psi^* = 0{\cdot}007$ and 0·014. Symbols are shaded in figures 4

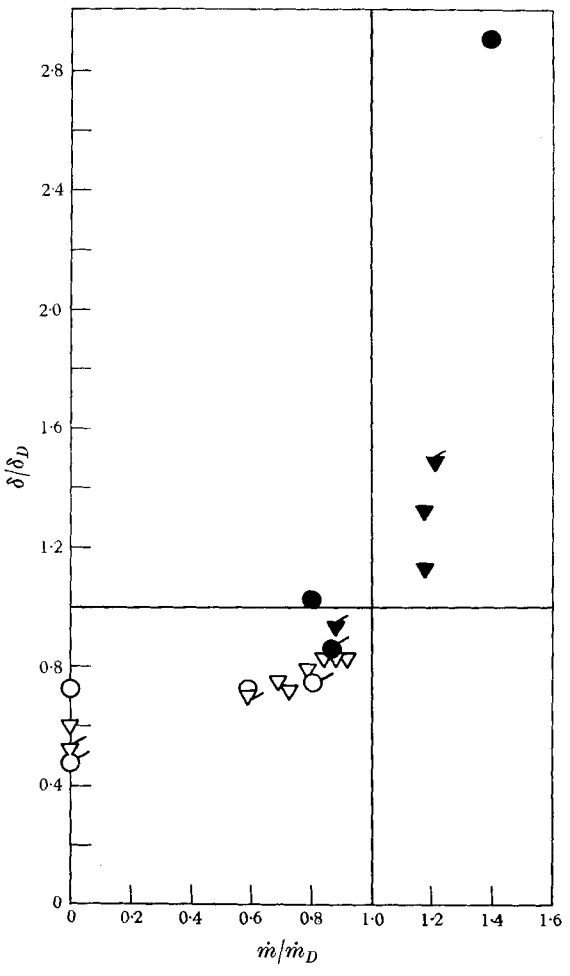

FIGURE 4. Shock-displacement-distance variation with injection rate, relative to design values. ○, $\psi^* = 0{\cdot}007$; ▽, $\psi^* = 0{\cdot}014$. Unflagged, model 1; flagged, model 2. Shaded symbols imply visibly overblown in shadowgraph picture.

and 5 to indicate observed overblown cases in the shadowgraphs. Shock displacement is finite without injection, increases at first slowly, then rapidly to the design condition ($\dot{m}/\dot{m}_D = \delta/\delta_D = 1{\cdot}0$) and subsequently levels off such that small increases in injection rate substantially affect δ/δ_D. Contact-surface displacement shows a similar behaviour but originates at the origin

$$(\dot{m}/\dot{m}_D = \Delta/\Delta_D = 0).$$

4. Discussion

The primary purpose of this investigation was a verification of the existence of a hemispherical contact surface brought about by injection through a properly contoured blunt nose. Despite inaccuracies resulting from small model dimen-

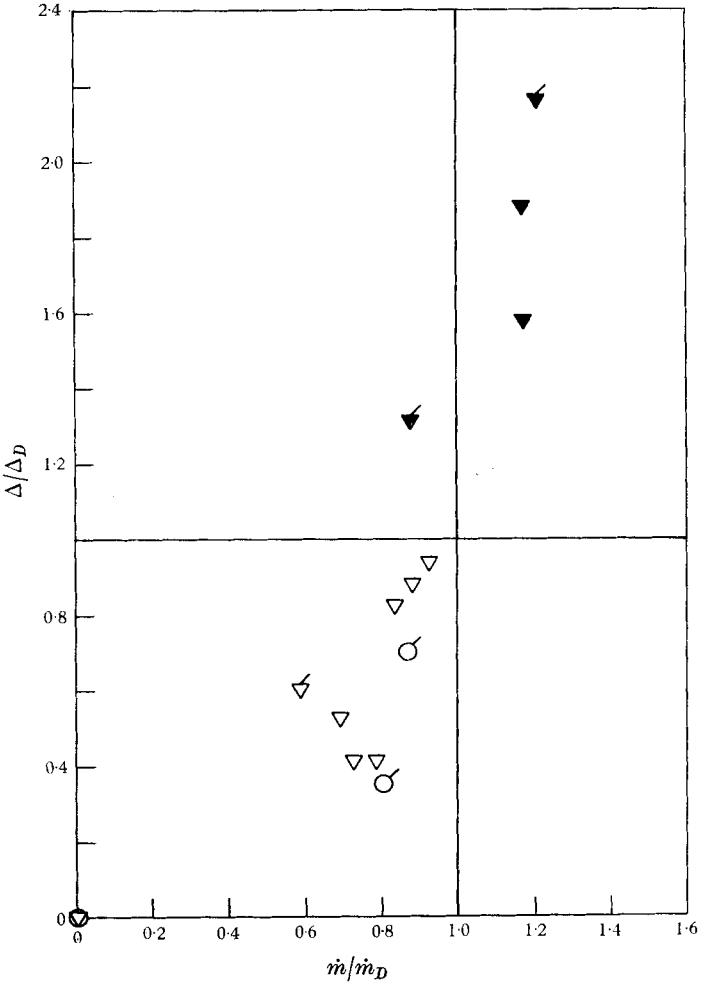

FIGURE 5. Contact surface-displacement-distance variation with injection rate relative to design values. ○, $\psi^* = 0{\cdot}007$; ▽, $\psi^* = 0{\cdot}014$. Unflagged, model 1; flagged, model 2. Shaded symbols imply visibly overblown conditions in shadowgraph picture.

sions it is believed that the photographic evidence bears out the conjecture. Although viscous effects must be present at the contact surface they were not appreciable for the test conditions. While the overblown case of a distorted bow shock is associated with flow rates $\dot{m} \gtrsim \dot{m}_D$ a major breakdown of the flow pattern does not occur until appreciably higher injection rates (compare figures 2*c* and 3*f*). This suggests that precise values of mass injection are not critical in any application to be made.

Air was injected during these tests for convenience. In future heat-transfer investigations of this two-layer model, use will be made of coolants of larger thermal capacities.

The research reported on above was sponsored by the U.S. Air Force Office of Scientific Reseach under Contract No. 49 (638)-245.

REFERENCES

MARTIN, E. D. 1958 Inviscid hypersonic flow around spheres and circular cylinders. *AFOSR TN*-58-448.

MCMAHON, H. M. 1958 An experimental study of the effect of mass injection at the stagnation point of a blunt body. *Calif. Inst. Tech. Guggenheim Aero. Lab. Hypersonic Res. Proj. Memo.* no. 42.

WARREN, C. H. E. 1960 An experimental investigation of the effect of ejecting a coolant gas at the nose of a bluff body. *J. Fluid Mech.* **8**, 400.

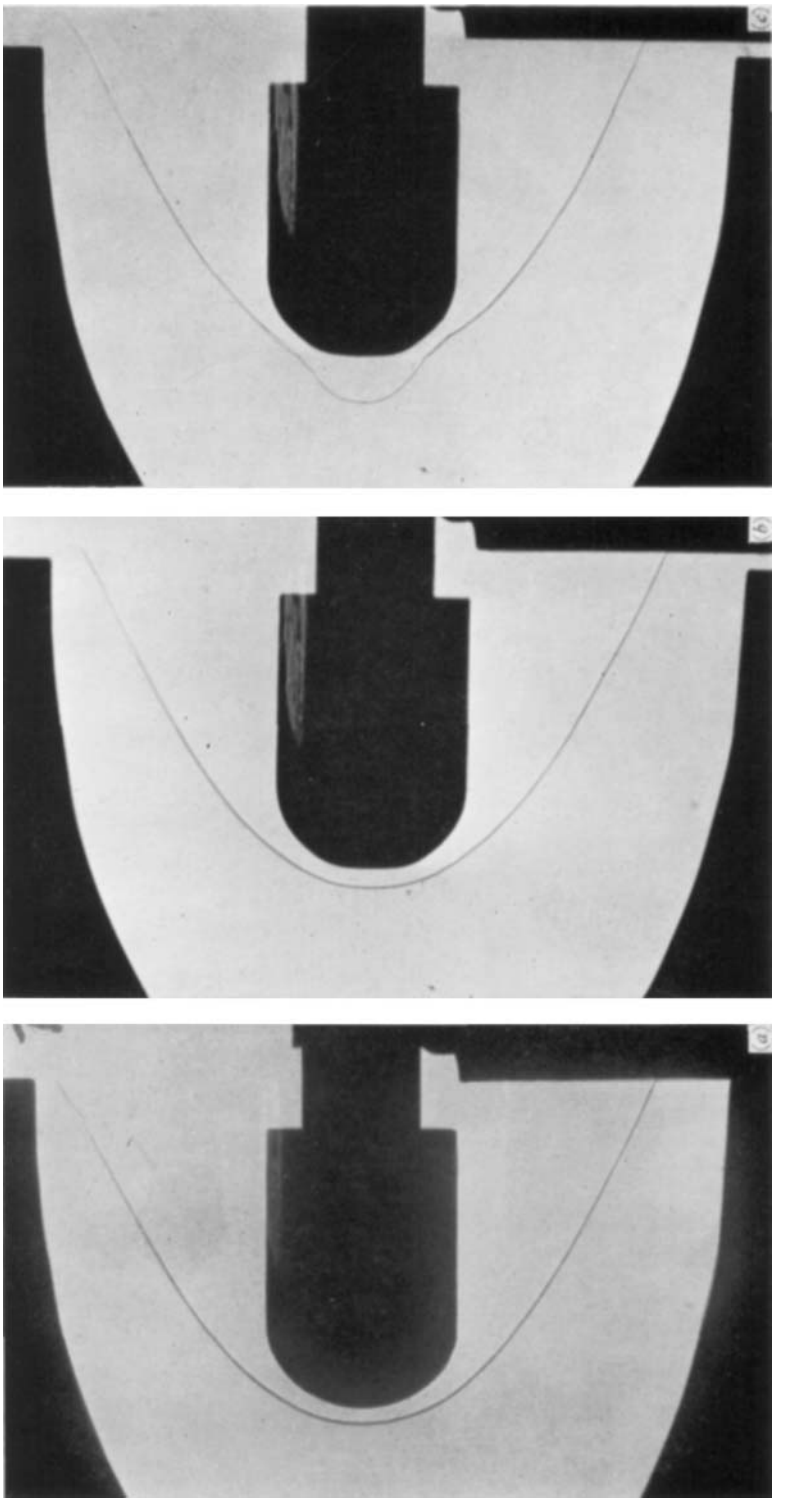

FIGURE 2, plate 1. Shadowgraphs, model 1. (*a*) $\psi^* = 0$; (*b*) $\psi^* = 0{\cdot}007$, $\dot{m}/\dot{m}_D = 0$; (*c*) $\psi^* = 0{\cdot}007$, $\dot{m}/\dot{m}_D = 1{\cdot}40$.

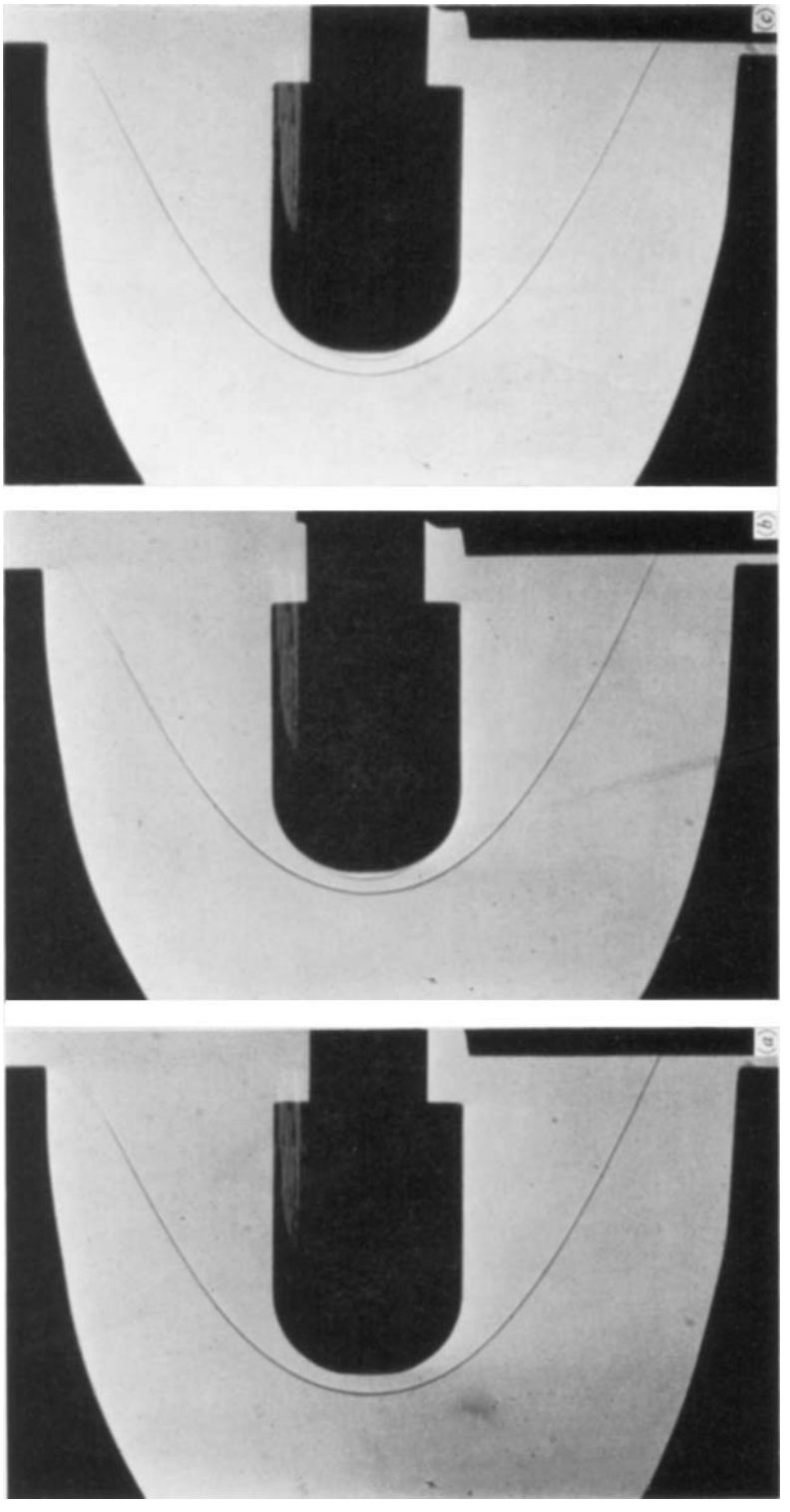

For legend see plate 3.

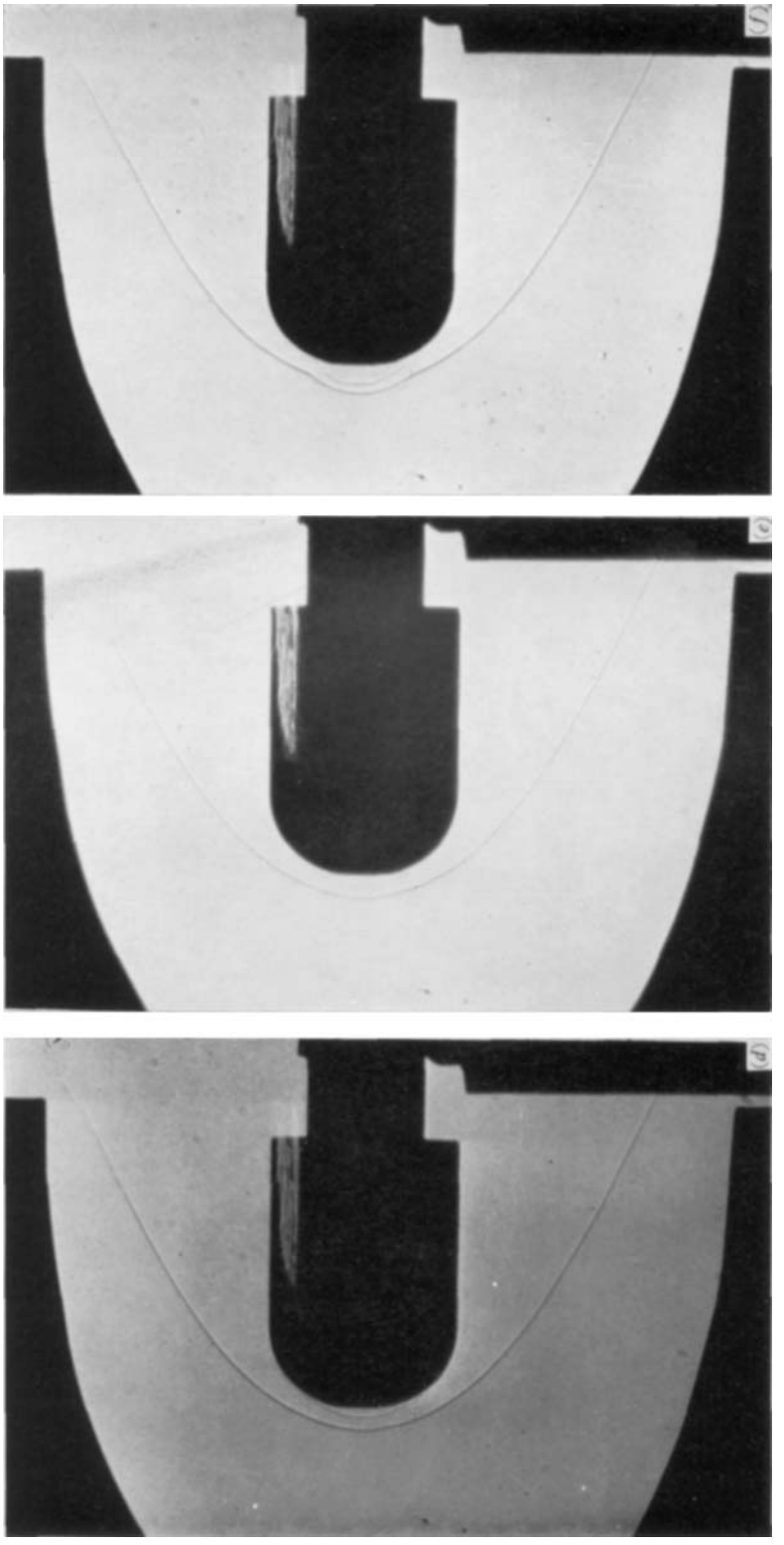

FIGURE 3, plates 2 and 3. Shadowgraphs model 1*c*, $\gamma^* = 0{\cdot}014$, $\dot{m}/\dot{m}_D =$ (*a*) 0; (*b*) 0·689; (*c*) 0·785; (*d*) 0·881; (*e*) 0·924; (*f*) 1·177.